An ALS Assembly Modulator Signature in Peripheral Blood Mononuclear Cells: Implications for ALS Pathophysiology, Therapeutics, and Diagnostics

Shao Feng Yu[1], Maya Michon[1], Anuradha F. Lingappa[1], Kumar Paulvannan[1], Dennis Solas[1], Kim Staats[2], Justin Ichida[2], Debendranath Dey[1], Jeffrey Rosenfeld[3] and Vishwanath R. Lingappa[1,4,5]

[1] Prosetta Biosciences, Inc. 670 5th St San Francisco, CA 94107

[2] University of Southern California, Los Angeles, CA 90033

[3] Loma Linda Medical Center, Loma Linda, CA 92354

[4] Department of Physiology, University of California, San Francisco, CA 94143

[5] To whom correspondence should be directed (vlingappa@prosetta.com)

Abstract

Assembly modulators are a new class of allosteric site-targeted therapeutic small molecules, some of which are effective at restoring nuclear localization of TDP-43 in ALS cellular models, and which display efficacy in a variety of ALS animal models. These compounds have been shown to bind selectively to a small subset of protein disulfide isomerase (PDI), a protein implicated in ALS pathophysiology. The targeted subset of PDI is found within a novel, transient and energy-dependent multi-protein complex that includes other important members of the ALS interactome, such as TDP-43, RanGTPase, and selective autophagy receptor p62/SQSTM1. We demonstrate here that a similar multi-protein complex drug target is present in PBMCs as isolated by energy-dependent drug resin affinity chromatography (eDRAC) and characterized by mass spectrometry and by Western blot (WB). Signature alterations in the composition of the multi-protein complex in PBMCs from ALS patients compared to PBMCs from healthy individuals were identified by WB of eDRAC bound proteins, thereby extending earlier literature suggesting PBMC dysfunction in ALS. Changes in the PBMC drug target in ALS patients compared to healthy individuals include diminished p62/SQSTM1 and appearance of a 17kDa post-translationally modified form of RanGTPase. These changes are not readily apparent from analysis of whole cell extracts, as the individual protein components within the drug target multi-protein complex comprise only small percentages of the total of those component proteins in the extract. Furthermore, whole blood from ALS patients shows a distinctive degradation of total RanGTPase not observed in blood from healthy individuals. This degradation appears to be rescued by treatment of whole blood from ALS patients for 72 hrs with ALS-active assembly modulator small molecules. Our findings are consistent with the hypothesis that ALS is

45 fundamentally a disorder of homeostasis that can be detected early, prior to disability, in blood
46 by the methods described, and restored to the healthy state by assembly modulator drug
47 treatment.
48
49 **Introduction**
50 Amyotrophic Lateral Sclerosis (ALS) is a devastating neurodegenerative disease that
51 strikes approximately 6,000 American and 150,000 people worldwide annually[1,2]. Approximately
52 10% of ALS is familial, with a large number of specific gene mutations implicated. The vast
53 majority of ALS cases however, are sporadic, meaning that that there is no family history of the
54 disease and therefore seems likely due to an environmental cause, perhaps with epigenetic
55 influence[3]. Specific environmental factors have been implicated in causing ALS, but remain
56 controversial and inconclusive[4]. While the pathophysiology of ALS is not well understood,
57 aggregates of the protein TDP-43, independently implicated in the HIV life cycle[5], are almost
58 invariably found in the brains of patients with ALS and fronto-temporal dementia (FTD)[6].
59 Despite this commonality, the clinical presentation as well as progression of ALS, is highly
60 variable[7].
61
62 With regards to TDP-43 pathophysiology, controversy exists as to the triggering event.
63 Some studies have implicated mislocalization of TDP-43 from the nucleus in healthy cells to the
64 cytoplasm, which is observed to variable degrees in fibroblasts from many, but not all, cases of
65 ALS[8]. An alternative view is that, in response to stress, TDP-43 forms aggregates in the
66 cytoplasm where it is synthesized, prior to transport to the nucleus[9]. A further controversy

67 exists as to whether the relevant TDP-43 aggregates in the cytoplasm are within, or outside of,
68 stress granules[10]. While the TDP-43 aggregates have generally been viewed as a trigger of motor
69 neuron death, it is possible that they are an epiphenomenon whose elimination *per se* may not
70 necessarily be therapeutic, by analogy to the failed attempts to remedy Alzheimer's Disease by
71 elimination of Aβ aggregates[11]. Regardless of their natural history and role in the
72 pathophysiology of ALS, the presence of TDP-43 aggregates are pathognomonic for the
73 disease[12,13].
74
75 Recently we presented our studies on the role of a newly appreciated dimension of gene
76 expression, termed protein assembly, in the pathophysiology of diverse diseases including
77 ALS[14,15,16]. These compounds were found by a novel method in which viruses were used as
78 "trufflehounds" to reveal drug targets inaccessible by genomic or conventional proteomics[15,16].
79 We have identified several structurally unrelated small molecule chemotypes by virtue of their
80 ability to modulate host machinery catalytic for viral capsid formation, that we term protein
81 assembly modulators. These compounds are strikingly efficacious both for the specific viral
82 disease by which they were identified, and also for a subset of non-viral diseases. Among the
83 protein assembly modulators with activity against HIV, one prevents ALS-associated
84 neurodegeneration and its correlates in various cellular and animal models of ALS[14]. A subseries
85 of analogs shows diminished activity against HIV and improved activity against ALS. These
86 compounds are broadly effective at reversing both TDP-43 mislocalization and stress-induced
87 TDP-43 aggregation, in both familial and sporadic ALS and fronto-temporal dementia (FTD)
88 cellular models. Efficacy has also been demonstrated in various transgenic animals expressing

89 human ALS-causing mutations including in TDP-43, FUS, c9orf72, and SOD1, by a variety of
90 assays[14]. In view of this breadth of efficacy, we hypothesized the drug target to be a step
91 common to most, if not all, ALS and FTD. Advanced analogs of the ALS-selective active subseries
92 of one of these chemotypes are close to completion of a target product profile (TPP), prior to
93 initiation of investigational new drug (IND)-enabling studies in anticipation of human clinical
94 trials in the near future.
95
96 The studies to be described here had several motivations. First, to explore the
97 hypothesis that the biochemical pathways involved in ALS pathophysiology may involve layers of
98 regulation yet to be discovered[17,18], in which the novel multi-protein complex targets of these
99 compounds might be involved. How those levels of control are integrated with one another,
100 and are communicated from one organ system to others, remain largely unknown. It may be
101 that the novel assembly modulator targets we have discovered are potential candidates for
102 involvement in such regulation. By corollary, what happens to other feedback controls when
103 one level of regulation fails, remains to be determined. The argument has been made based on
104 gene knockout experiments that more ancient back up pathways may be activated when
105 primary regulatory controls fail[19,20]. Having a drug that impinges on a biochemical pathway in a
106 novel way is a powerful means of probing biological regulation. Much of this regulation depends
107 on information that does not reside simply in the sequence of the genome[18,20,21]. Thus the
108 relevance of the compounds we describe, with their unconventional multi-protein complex
109 target (energy-dependent for formation, transient in existence, composed of miniscule subsets
110 of the individual component proteins in the cell), and novel mechanism of action at allosteric

111 sites[22,23 24,25]. These tools may provide a new understanding of the molecular basis for
112 homeostasis, and its dysregulation, as exemplified in ALS.
113
114 A second motivation for the present studies was to understand the meaning of the
115 observed dysfunction of PBMCs in ALS[26,27]. These findings can be interpreted in very different
116 ways. On the one hand, PBMC dysfunction might be due to ALS being a systemic disease whose
117 most severe manifestation is motor neuron death, but which also manifests in less dramatic
118 fashion in other organ systems, including in blood. Alternatively, the signature observed in
119 PBMCs might reflect a role of blood, which sees essentially every cell in the body on a regular
120 basis, spreading the message that there is a disorder affecting a particular cell type, in this case,
121 motor neurons. Yet another possibility is that the disorder affecting one organ system (motor
122 neurons) could have a "domino effect" manifesting in other organ systems (PBMCs), e.g. as a
123 secondary consequence of feedback regulation intended to monitor and maintain
124 homeostasis[17,28]. Prion-type spread observed for various diseases may be an example of such
125 disordered communication[28–30]. To better understand these alternatives, we asked whether
126 assembly modulator drugs might detect a version of the disordered drug target in PBMCs from
127 ALS patients.
128
129 Finally, apart from intellectually interesting questions of feedback and mechanism of
130 action[17,28,30], there is a practical desire to advance these compounds to the clinic, given their
131 remarkable therapeutic properties in cellular and animal models of ALS[31]. Having a readily
132 accessible signature of ALS in PBMCs would facilitate ALS drug advancement in innumerable

133 ways, most importantly by making possible early detection of ALS (prior to severe disability).
134 Compounds designed to restore homeostasis would be expected to be most effective when
135 administered early, before motor neuron death. Or put another way, treatments that restore
136 homeostasis would be expected to be very different from those needed to regrow and replace
137 cells after they have died. A signature in PBMCs would also provide a biomarker for easy
138 assessment of therapeutic efficacy, and to determine when therapy could be stopped or might
139 need to be restarted.
140
141 **Results**
142 Blinded blood samples were obtained from ALS patients and healthy individuals, under
143 an IRB-approved protocol. The PBMCs were isolated, and extracts prepared as described in
144 methods, and analyzed for key proteins relevant to ALS. Differences observed in the protein
145 pattern between PBMCs of healthy and ALS patients, by total protein silver stain were subtle
146 (see for example, **Figure 1A**).
147 However when PBMC extracts were applied to the ALS-active drug resin described
148 previously[31] versus control resin (lacking the drug ligand), washed and bound material analyzed,
149 a distinctive subset of proteins was observed, also largely shared between healthy individuals
150 and ALS patients, but with a few possible differences (black arrows in **Figure 1B**).
151 Previous studies of assembly modulator small molecules[15,16] have shown that the
152 proteins comprising the multi-protein complex drug target represent single digit percent of the
153 total of those proteins in the starting extract. As expected therefore, the depleted extracts differ

very subtly from the starting material, as demonstrated for PBMC DRAC flow through here (see also **Supplemental Figure 1D**).

Figure 1

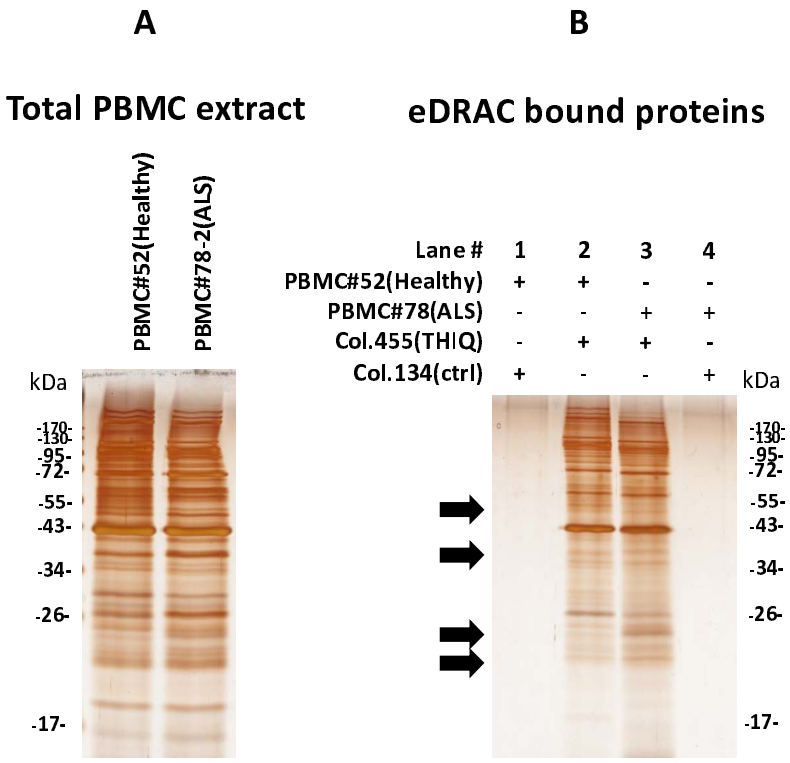

Legend to Figure 1. A. Silver stain of starting PBMC extract 10kxg/10min supernatant from a representative healthy individual (#52) and an ALS patient (#78-2). B. Silver stain of free drug eluate from ALS-active assembly modulator drug resin (column 455 THIQ) or control resin (column 134 lacking the drug ligand). Black arrows indicate positions at which healthy vs ALS patient samples show a suggestive difference in the free drug eluate protein pattern.

Mass spectrometry analysis of free drug eluates from PBMCs applied to the ALS-active drug resin (**Figure 2**) was carried out and compared to the pattern previous revealed from mouse brain (MoBr). A substantial proportion of tissue-specific proteins (~1/2 to 2/3 depending on the

166 specific sample) were observed (see **Supplemental Figure 2**). Despite the high tissue specificity,
167 a core set of 33 proteins shared between both PBMCs and brain were of interest. Of these, 26
168 were identified as members of the ALS protein interactome. Notably, this set included P4HB, a
169 member of the PDI family, two known ALS-causing proteins (TUBA4A and VCP)[32], along with
170 proteins implicated in the KEGG ALS interactome[33] (ATP5A1, HSPA5, TUBA1A, TUBA4A, and
171 VCP). Furthermore, 24 of these 33 proteins exhibited high-confidence interactions with known
172 ALS-causing or disease-modifying proteins[32]. The 26 shared ALS interactome proteins also
173 included multiple members of several protein families and complexes: two ATP synthase
174 subunits (ATP5A1 and ATP6V1A), six chaperonins containing T-complex components (CCT2,
175 CCT3, CCT4, CCT5, CCT7, and CCT8), three thioredoxin domain proteins (P4HB, PRDX1, and
176 PRDX2), and four members of the 14-3-3 family (YWHAB, YWHAE, YWHAH, and YWHAQ) (**Figure**
177 **2A**).
178
179 MCL clustering analysis was performed on the 33 shared proteins using the STRING
180 database, which integrates information from various databases cataloging known and predicted
181 protein-protein interactions. The analysis generated groups called "clusters," characterized by a
182 higher density of predicted associations within the clusters compared to those between
183 clusters. Notably, 31 out of the 33 proteins formed a single, highly interconnected cluster,
184 suggesting potential functional relationships between them. Two proteins, VAT1 and ALDH1A1,
185 were excluded from this cluster, as there are no predicted interactions between these proteins
186 and the other 31 proteins (**Figure 2B**). These findings are summarized in **Figure 2C.**
187

188

Figure 2

A

	WT mouse THIQ eluate	WT mouse Control eluate	SOD mouse THIQ eluate	SOD mouse control eluate	Healthy PBMC 44 THIQ eluate	Healthy PBMC 52 THIQ eluate	ALS PBMC 43 THIQ eluate	ALS PBMC 53 THIQ eluate	ALS PBMC 43 Control eluate	Causitive genes	Associated and disease modifier genes	ALS protein binding partners	KEGG ALS interactome
ACTN4	7	0	4	0	64	69	78	69	0				
ALDH1A1	2	0	7	0	8	0	0	2	0				
ATP5A1	22	0	17	0	2	5	5	6	0				
ATP6V1A	13	0	7	0	3	0	5	0	0				
CALM1	11	0	10	0	13	13	11	12	0				
CCT2	8	0	13	0	7	0	3	0	0				
CCT3	6	0	2	0	8	2	6	2	0				
CCT4	3	0	6	0	8	0	3	2	0				
CCT5	9	0	8	0	9	2	5	0	0				
CCT7	4	0	6	0	8	0	4	0	0				
CCT8	8	0	7	0	11	0	7	2	0				
EEF1G	9	2	10	0	4	4	5	2	0				
HSP90AA1	37	0	44	0	20	13	15	11	0				
HSP90AB1	39	0	46	0	19	15	15	8	0				
HSPA5	11	0	15	0	0	7	0	0	0				
HSPB1	4	0	6	0	4	17	10	0	0				
HSPD1	38	2	38	0	12	21	12	9	0				
LDHB	7	0	0	0	14	0	12	0	0				
P4HB	16	0	23	0	54	48	64	43	0				
PRDX1	8	0	11	0	8	6	4	4	0				
PRDX2	7	0	10	0	18	8	9	19	0				
ST13	6	0	11	0	3	0	4	5	0				
STIP1	32	0	35	0	3	9	0	0	0				
TCP1	6	0	5	0	6	0	4	0	0				
TUBA1A	17	0	15	0	10	12	15	18	0				
TUBA4A	16	3	12	0	11	14	18	18	0				
USP5	12	0	23	0	5	0	2	0	0				
VAT1	9	0	10	0	4	0	10	3	0				
VCP	47	2	53	0	55	62	58	55	0				
YWHAB	9	0	0	0	12	6	9	0	0				
YWHAE	9	0	11	0	6	6	6	0	0				
YWHAH	6	0	7	0	6	7	8	0	0				
YWHAQ	10	0	9	0	0	5	6	7	0				

B

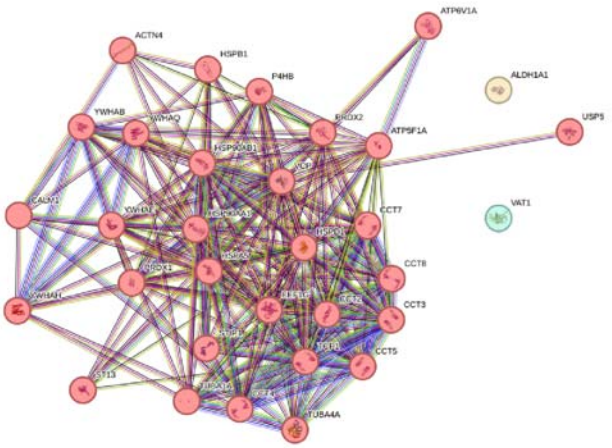

189

190

C

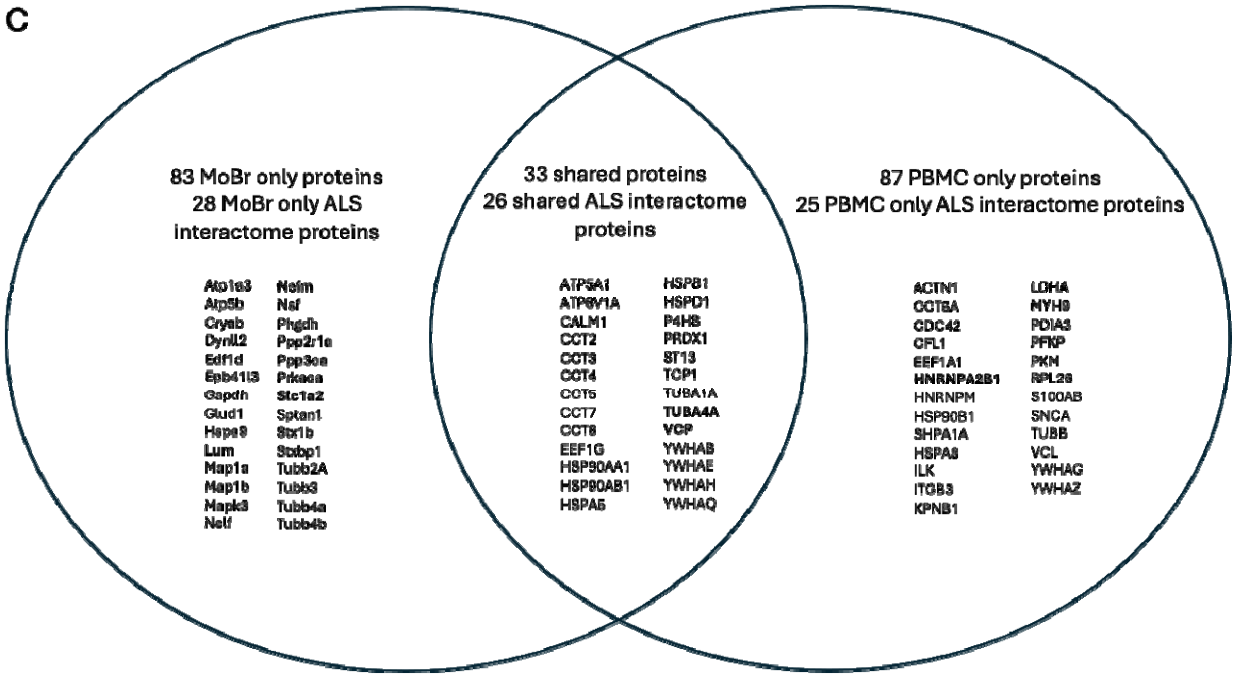

191

192 Legend to Figure 2. A. Spectral counts for proteins identified in THIQ drug resin eluate from MoBr and

193 human PBMC extracts. Colors represent the number of spectral counts for a given protein in each

194 sample, ranging from light green (low counts) to dark green (high counts). The right panel indicates "hits"
195 for proteins present in the ALS interactome, where yellow is a hit. B. STRING database protein-protein
196 interaction network with MCL clustering. Each circle ("node") represents a protein, and each line
197 ("edge") represents a predicted interaction between two nodes. Different colors represent distinct
198 clusters identified by the MCL algorithm, with red indicating the largest cluster and yellow and green
199 representing clusters containing only a single protein. C. ALS interactome proteins identified by MS-MS
200 are shown in venn diagram. Causative and disease modifier proteins are in **bold**.
201
202 From the MS-MS analysis it was clear that the multi-protein complex isolated from
203 PBMCs on the ALS-active drug resin appears related to that observed in MoBr, based on the 27
204 shared proteins identified that are in the ALS protein interactome observed from both sources.
205 However no clear differences between healthy and ALS patients were observed by MS-MS.
206
207 Recognizing that MS-MS analysis as carried out here can fail to identify specific proteins
208 for a number of reasons, including covalent post-translational modifications (PTMs) that alter
209 peptide mass, or result in failure of peptide cleavage with trypsin and/or ionization, we analyzed
210 the DRAC bound material by WB to identify particular proteins of interest. WB has its own
211 limitations, partially but not completely overlapping with those of MS-MS. A shared limitation
212 with MS-MS is that a covalent post-translational can mask an epitope making it undetectable by
213 an epitope-specific antibody. Nevertheless, if a difference between healthy and ALS patients in a
214 protein within the drug resin-bound target complex were identified either by WB or MS-MS, it
215 could serve as a signature of the disease. From WB of the DRAC bound material two proteins
216 were strikingly different between most healthy individuals studied and most ALS patients. First,

217 p62/SQSTM1, a known regulator of autophagy, an important host defensive mechanism, was
218 greatly diminished in ALS patient PBMC DRAC free drug eluates compared to that from most
219 healthy individuals. Conversely, a 17kDa post-translationally modified fragment of RanGTPase
220 was detected in ALS patients, but not in most healthy individuals, in DRAC free drug eluates. A
221 representative example is shown in **Figure 3**.

222 **Figure 3.**

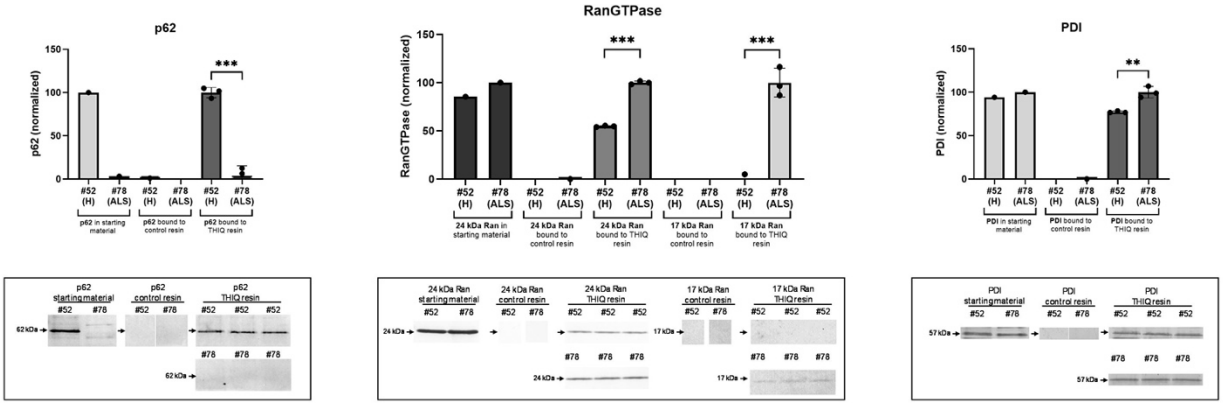

223

224 Legend to Figure 3. PBMC extracts were prepared from ALS patients (ALS) or healthy individuals (H) as
225 described in methods and applied to drug resin versus control resin, washed and bound proteins
226 analyzed by SDS-PAGE transferred to 0.2u PVDF membrane and WB for the indicated proteins (below)
227 with quantitation of bands using Image J software (above). Shown is DRAC bound material from a
228 healthy control (#52) and a sporadic ALS patient (#78) analyzed by WB for p62/SQSTM1, RanGTPase, and
229 PDI. The highest value in each healthy/ALS graph pair is normalized to 100% for proportional
230 comparison to the lower value.

231

232 Out of 13 ALS patients and 6 healthy controls assessed in a blinded fashion, all 13 ALS
233 patients had a strikingly low values for p62 in the drug resin bound material. Of the 6 healthy
234 controls, 2 were low. For Ran 17 kDa fragment, all 13 ALS patients had a higher value than the

235 parallel reference healthy control. Among the 6 healthy controls, the two with low p62 also had
236 high Ran 17 kDa fragment in the eDRAC bound material. In contrast to striking loss of p62 and
237 appearance of RanGTPase 17kDa fragment, only a modest difference in the direct drug-binding
238 protein, PDI, was observed between ALS patients and healthy controls.
239
240 Thus, taken together, the eDRAC signatures observed appear to have a sensitivity
241 approaching 100% and a specificity of approximately 66% for ALS, albeit from a modest sample
242 size. Further studies are needed to understand how these differences come about and what
243 their significance is to the underlying pathophysiology of ALS. Nevertheless, together with the
244 clinical picture, they suggest a basis for early detection of ALS using as an affinity ligand, a small
245 molecule that is therapeutic for the disease in a diversity of animal models studied[14]. **Table 1**
246 summarizes these findings together with key demographic features of the individuals studied.
247 The eDRAC signature in PBMCs, like that observed previously in other cells and tissues,
248 represent very small subsets of the total of the proteins in the target multi-protein complex
249 (**Supplemental Figure 3**).
250
251

	% p62	% 17kDa Ran Fragment	sex	age at onset	age dx	age at presentation	date of death	disease course	sample date (mo/day/yr)
#52 (healthy)	100 (650)	1 (2)	F			41			7/31/18
#40 (ALS)	71 (462)	5 (12)	M	68	71	72	N/A	LMN predominant - early bulbar/trach slow, progressive course	1/24/19
#50 (ALS)	30 (193)	12 (32)	M	46	47	59	10/21/22	Generalized slowly progressive disease	7/31/18 1/24/19
#51 (ALS)	64 (419)	8 (22)	M	38	39	40	3/1/23	UMN predominant generalized disease with bulbar compromise	7/31/18
#68 (ALS)	3 (16)	100 (261)	F	78	79	79	N/A	primary bulbar presentation with mostly UMN features	2/19/19
#54 (ALS)	6 (41)	76 (197)	M	51	52	52	2/5/19	rapidly progressive, bulbar involving disease	8/7/18
#55 (healthy)	10 (63)	86 (224)	F			55			
#52 (healthy)	80 (645)	0 (0)	F			41			7/31/18
#45 (ALS)	13 (64)	61 (63)	M	42	43	43	N/A		5/22/18 2/28/19
#78 (ALS)	6 (35)	100 (103)	F	45	46	46	10/7/20	LMN predominant, generalized disease	5/28/19 7/18/19
#52 (healthy)	99 (700)	8 (8)	F			41			7/31/18
#87 (healthy)	100 (706)	5 (5)	M			36			12/19/19
#52 (healthy)	100 (710)	0 (0)	F			41			7/31/18
#43 (ALS)	12 (85)	100 (44)	F	68	71	72	12/19/18	UMN predominant; generalized disesease with significant bulbar compromise	12/19/18
#44 (healthy)	15 (105)	27 (12)	F			74			
#46 (ALS)	54 (385)	11 (5)	M	53	54	54	N/A	bulbar onset then generalized disease	5/23/18
#47 (healthy)	56 (400)	7 (3)	M			58			
#53 (ALS)	0 (0)	68 (30)	F	67	68	71	2/12/19	limb onset generalized disease, possible concurrent Parkinson's disease	7/31/18
#26 (healthy)	100 (558)	0 (0)	M			64			1/22/18
#34 (ALS)	1 (3)	7 (2)	M	40	42	42	N/A	monomelic presentation VERY slow LMN generalization, bulbar sparing	2/15/18
#69 (ALS)	2 (13)	100 (24)	M	80	82	82	5/8/21	LMN predominant, generalized disease	2/19/19
#70 (ALS)	13 (71)	7 (2)	M	42	42	43	N/A	generalized progressive disease	2/28/19

Legend to Table 1. 13 ALS patients and 6 healthy controls were analyzed over 4 separate experiments and the data tabulated, together with key demographic and clinical history information. For each experiment the highest value p62 was set at 100% and the others scaled proportionally. Likewise, in each experiment the highest value 17kDa Ran fragment was set at 100% and the others scaled proportionally. The quantified WB band value is also shown in parentheses. Healthy individuals are noted in green, and ALS patients in red, except for the two healthy individuals displaying the ALS phenotype, whose values are in black.

261 Next, photocrosslinking was carried out with PBMC extracts to which was added a drug
262 analog in which the attachment to resin was replaced by attachment to a biotin and diazirine
263 moiety such that exposure to UV light results in a covalent linkage to the drug binding
264 protein(s). Under native conditions associated proteins of the entire multi-protein complex can
265 be precipitated with streptavidin beads. If the sample is first denatured, then only the direct
266 drug-binding protein will be precipitated with streptavidin beads under the conditions
267 described. Figure 4 demonstrates that PDI is the direct drug-binding protein. It should be noted
268 that P4HB found by MS-MS is the gene name for the same PDI family member detected by the
269 PDI antibody by WB.
270

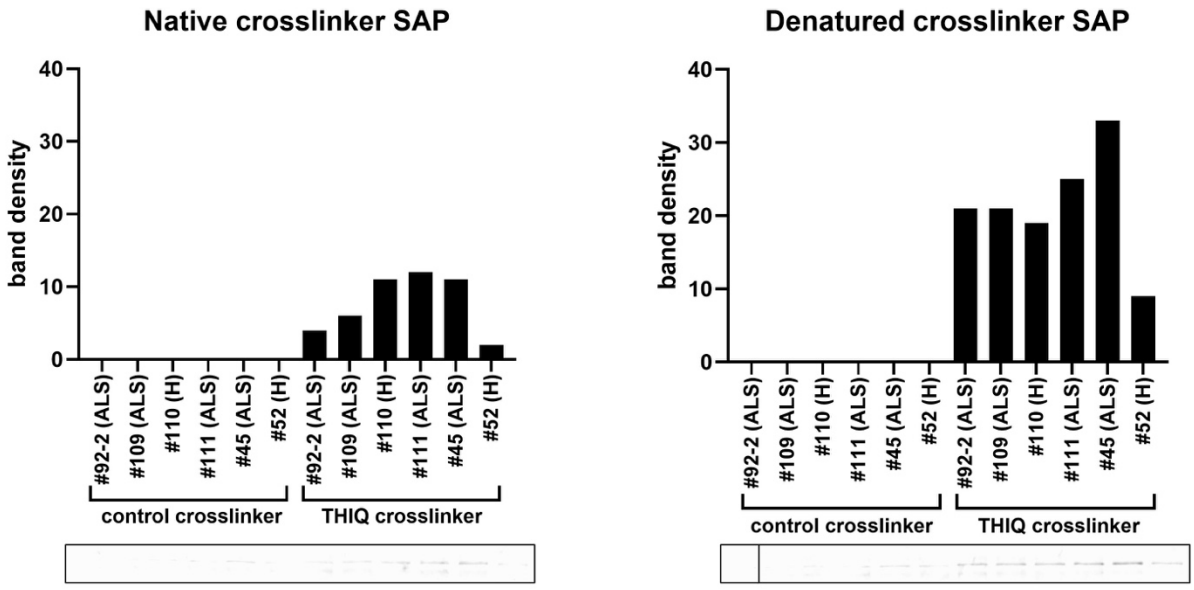

271

272 Legend to Figure 4. Quantitation of PDI in streptavidin precipitates from PBMC extracts prepared from
273 ALS patients (ALS) or healthy individuals (H), under native vs denatured conditions after
274 photocrosslinking with PAV-073 analog (THIQ) or control crosslinker lacking the drug ligand. Both control
275 and THIQ crosslinkers contain biotin and diazirine as described in methods and previously[31].

We then assessed whether the ALS patient vs healthy control correlations involving p62 and Ran 17kDa fragment, as shown in **Figure 3** and **Table 1**, were accentuated over time with progression of ALS. As can be seen in **Figure 5**, with progression of disease, the amount of PBMC p62 bound to the resin, which is much higher in healthy individuals (panel A), diminishes with advancement of ALS. In parallel, the amount of the RanGTPase 17kDa fragment, which is missing in PBMCs from healthy individuals, increases with ALS disease progression.

Notably, the diagnosis of ALS was made in pt 78 very early in her disease progression. She was able to drive herself to the clinic and walk in with a cane, at the time that the initial blood sample was taken, which nevertheless revealed the dual signatures of falling p62 and appearance of Ran 17kDa fragment, in contrast to parallel analysis of a healthy control. As will be seen these features appear to be exacerbated with disease progression.

Figure 5.

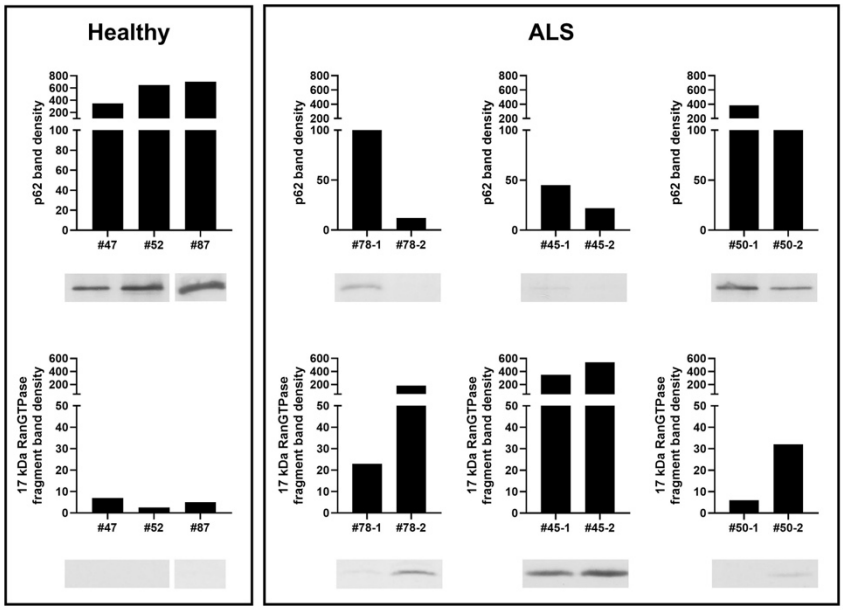

Legend to Figure 5. PBMC extracts were prepared as previously, applied to drug resins and bound proteins analyzed by WB for specific proteins of interest. Bands corresponding to the correct molecular weights were quantified. Blood samples from three ALS patients were assessed over time for both p62 and RanGTPase 17kDa fragment bound to DRAC. Timing of blood draws were 6 weeks apart for patient 78, 6 months apart for patient 50, and 9 months apart for patient 45.

291

292 If, as we suggest, ALS represents a breakdown in homeostasis where protective
293 mechanisms to reboot a cellular operating system are ineffective, certain predictions follow. For
294 one, there may be a backup mechanism activated in an attempt to correct the failure of the first
295 line of defense, although by definition, in patients who progress to ALS, that backup has failed
296 to correct the problem. By analogy, when your computer is frozen (with appearance of the
297 "colored wheel of doom"), simply attempting to undo the key stroke that caused it to freeze will
298 not be effective. Instead, it is necessary to reboot the operating system. Perhaps assembly
299 modulators provide precisely such a biochemical reboot of the cellular operating system. In
300 view of the distinctive ALS-associated appearance of a 17kDa fragment of RanGTPase, as noted
301 in **Figure 5** above, degradation of RanGTPase, seemed like a plausible backup feedback
302 response. This backup feedback response would be engaged if less draconian feedback methods
303 failed.

304

305 A second prediction is that if, as we hypothesize, assembly modulation is a fundamental
306 mechanism of regulation of gene expression, and its activation by these compounds is
307 therapeutic for ALS, treatment of whole blood from ALS patients with the drugs should result in
308 cessation of the backup RanGTPase degradation feedback loop, upon "reboot" of homeostatic
309 control.

310

311 To test these hypotheses, we took blinded blood samples from ALS patients and healthy
312 controls and treated the whole blood with two different, structurally unrelated ALS therapeutic

assembly modulator compounds versus vehicle control (DMSO). Since RanGTPase is implicated in ALS pathophysiology and in the PBMC signature presented in Figures 3 and 5 we chose to assess a readily measurable potential feedback response: degradation of total RanGTPase, even though only a small subfraction of RanGTPase is hypothesized to be involved in ALS pathophysiology. We assessed the stability of RanGTPase with and without 72 hrs of assembly modulator treatment. After the 72 hr incubation of whole blood, RanGTPase stability in extracts was assessed in a 1hr incubation (**Figure 6**). In some samples, RanGTPase was observed to be stable over the course of a 1 hour incubation. These proved to be the healthy controls, when unblinded. However in blood from all of the ALS patients, the levels of RanGTPase after the 1hr incubation of whole blood extracts were greatly diminished, consistent with what would be expected for degradation of all RanGTPase as an extreme feedback response to the progression of ALS. Upon treatment with either of advanced analogs of two ALS assembly modulator chemotypes (called 073 and 667) for 72hrs, a striking diminution of RanGTPase degradation on subsequent 1hr extract incubation was observed, with no change in the level of RanGTPase observed in healthy subjects.

Figure 6

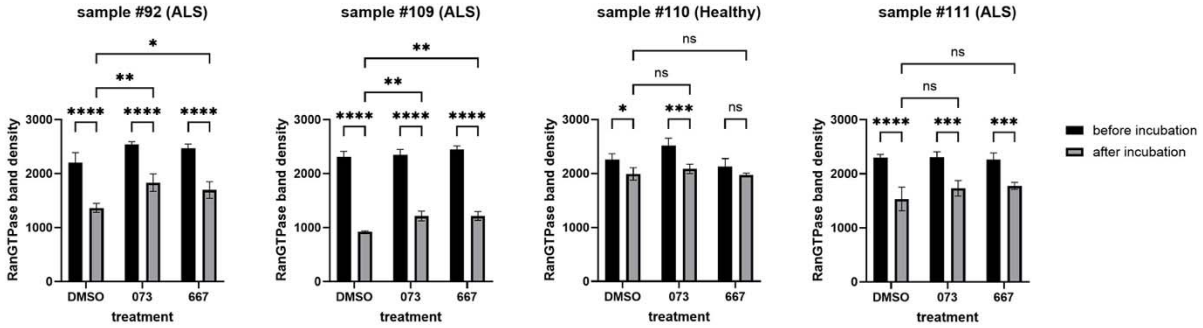

330 Legend to Figure 6. 10mls of whole blood from ALS patients or healthy controls was collected under an
331 IRB-approved protocol and shipped overnight at room temperature in EDTA-anticoagulated (purple top)
332 tubes without any patient-specific confidential information. An aliquot of whole blood was taken,
333 incubated in 1% SDS for one hour at 37°C, prepared for SDS-PAGE, and set aside. Another aliquot of
334 whole blood was mixed 1:1 with glucose-supplemented MEM and incubated for 72hrs at 37°C in the
335 presence of vehicle or protein assembly modulator drugs 073 and 667, at the end of which samples were
336 processed as previously described, and analyzed by SDS-PAGE. Black bars refer to the sample prepared
337 for SDS-PAGE immediately, while gray bars refer to the samples incubated prior to preparation for SDS-
338 PAGE.

Table 2

Analog representative of chemotype	Molecular weight (g/mol)	log P	H-bond donors	H-bond acceptors	Topological polar surface area (Å²)	Tanimoto similarity coefficient
PAV-073	443.543	4.8	1	5	49	<20%
PAV-667	441.915	6.4	0	7	73.7	<20%

Legend to Table 2. Two structurally unrelated (Tanimoto similarity coefficient <20 %) assembly modulator chemotypes used in the experiments shown in Figure 6 are compared for drug-like properties.

339

340

341 **Discussion**

342 The studies presented here demonstrate the presence, by energy-dependent DRAC and
343 photocrosslinking, of a multi-protein complex in PBMCs that is related to that observed
344 previously by the same methods in Tg ALS SOD G93A model MoBr and ALS patient-derived
345 fibroblasts (PDFs) that display both TDP-43 mislocalization and stress-induced agregation[14]. As
346 observed previously for the drug target in MoBr and PDFs, the multi-protein complex drug

347 target in PBMCs has a small subset of PDI as the direct drug-binding protein. The complex
348 present in ALS patient PBMCs also shares with the target in MoBr the presence of 26 proteins
349 implicated in the ALS interactome (Figure 2C). The precise role of this multi-protein complex
350 drug target in ALS pathophysiology remains to be determined. However, based on the efficacy
351 of structurally unrelated ALS assembly modulators in various cellular and animal models, we
352 hypothesize that the drug target serves a role in maintenance of homeostasis, whose loss
353 results in ALS. The presence of p62 in the complex in PBMCs from healthy individuals, and its
354 striking diminution in ALS patient PBMCs, exacerbated with disease progression (Figure 5), are
355 consistent with this hypothesis.
356
357 Likewise, the appearance of a 17kDa post-translationally modified form of RanGTPase in
358 the drug target isolated from ALS patient PBMCs (Figure 3 and Table 1) suggests a complex
359 biology connected to TDP-43 mislocalization, in view of the crucial role of RanGTPase in nucleo-
360 cytoplasmic transport. These changes appear very early in ALS, as suggested by their detection
361 in patient #78 prior to onset of significant disability (Figure 4). In the three cases where a
362 second sample was assessed 6 weeks to 9 months after the first blood draw, both signatures
363 were seen to be exacerbated with disease progression. These signatures had a sensitivity of
364 100%, detected in PBMCs of all 13 sporadic ALS patients studied, and a specificity of 66% for
365 distinguishing ALS patients from healthy individuals. While a larger number of cases will need to
366 be assessed, this early degree of discrimination, using as an affinity ligand a drug shown
367 therapeutically active in a diversity of animal models, is promising as a novel path to an ALS
368 biomarker and highly relevant to ALS therapeutics.

369

370 This target multi-protein complex is implicated in ALS for four reasons. First, the drug
371 that served as the ligand to bind and isolate the target is therapeutic in a wide range of ALS
372 cellular and animal models[31]. Second, the composition of the target multi-protein complex
373 includes a number of proteins of the ALS interactome, 26 of which are shared with the
374 corresponding complex in MoBr. Third, the isolated target from ALS patient PBMCs is altered in
375 protein composition compared to that from most healthy controls by two metrics: diminution of
376 p62/SQSTM1 and appearance of 17kDa fragment of Ran GTPase. Finally, separate from the
377 specific target in PBMCs, a profound degradation of total RanGTPase is observed in whole blood
378 from ALS patients but not in healthy controls, and is substantially rescued after 72hrs of
379 treatment with ALS-active assembly modulators.

380

381 We interpret these findings to suggest that ALS is, fundamentally, a disease of disrupted
382 homeostasis, for which assembly modulators may be therapeutic. By analogy to another
383 therapeutic area where assembly modulation treatment may be effective[16], it is notable that
384 the vast majority of individuals don't have cancer for most of their lives. However, a small
385 number will develop cancer, at least in part due to failure of homeostatic host defenses. So also
386 host defenses protect most of us most of the time from the consequences of various central
387 nervous system (CNS) insults, including those causing ALS. Host defenses, including restoration
388 of homeostasis, usually result in resolution of a CNS insult. Sometimes however, those host
389 defenses fail. As a result, homeostasis is not restored, and progression to motor neuron death is
390 accelerated. It seems reasonable to hypothesize that when initial feedback loops fail to restore

391 homeostasis, more and more severe feedback responses are triggered. Thus, mass degradation
392 of RanGTPase, as observed here in whole blood from ALS patients (Figure 6), may represent a
393 final desperate attempt to restore defective nucleocytoplasmic transport that results in TDP-43
394 mislocalization. Autophagy, in part mediated by p62/SQSTM1, is an example of a biochemical
395 reboot of the cellular operating system. When the reboot fails, e.g. in part due to loss of p62
396 from the dysfunctional target, the consequence in a subset of cases may be ALS. This persistent
397 deviation from homeostasis is a stress to which motor neurons appear highly sensitive, and
398 eventually, succumb. A drug capable of restoring homeostasis is likely most effective before
399 motor neurons have died, although perhaps synaptic plasticity could synergize allowing some
400 degree of recovery, once homeostasis has been restored. Regardless, it is surely a truism of
401 medicine that the earlier a disease is detected, the more effective most therapeutic
402 interventions are likely to be. Hence the importance of early detection to enable early
403 treatment, which the PBMC signatures noted here may provide.
404
405 The results of the whole blood experiments (Figure 6) are consistent with the hypothesis
406 that the degradation of total RanGTPase observed, is an extreme feedback response to the
407 inability more proximal and focused feedback loops to restore the target complex, comprised of
408 a small subset of RanGTPase, back to the healthy state. Treatment with either of two
409 structurally unrelated assembly modulators results in correction of the RanGTPase degradation
410 observed in whole blood, to a significant extent. We hypothesize that treatment for a longer
411 period would have completely restored RanGTPase levels to normal. Whether assembly
412 modulator drug treatment serves to fully reboot the system, e.g. restore p62 to the target

413 complex as has been observed for assembly modulation using a structurally unrelated molecule
414 in a different therapeutic area[15], remains to be determined and may vary on a case-by-case
415 basis. Likewise, further studies are needed to determine whether periodic or ongoing drug
416 treatment are required. Regardless, drug-induced changes in target composition, as implied by
417 stabilization of RanGTPase in ALS patient blood treated with assembly modulators, is consistent
418 with restoration of homeostasis. Whether this is reflective of concomitant changes in motor
419 neurons that prevent further motor neuron loss, remains to be investigated.
420
421 Our findings are significant for a number of reasons. First, these studies provide a
422 window into novel regulatory feedback loops involved in cellular homeostasis. The precise
423 relationship of the target multi-protein complex in healthy individuals vs ALS patients remains
424 to be more fully understood. One hypothesis is that the target multi-protein complex in healthy
425 individuals is the "normal" assembly machine involved in integration of diverse events of
426 homeostasis. These may include TDP-43 localization, in which RanGTPase likely plays a critical
427 role, perhaps along with C9orf72 and other ALS-implicated gene products. Other relevant
428 pathways, including autophagic removal of dysfunctional multi-protein complexes, are naturally
429 integrated into the physiological feedback that collectively bring about homeostasis. ALS may be
430 an example where a "stuck" pathway triggers more and more desperate feedback attempts to
431 reboot the system without success, culminating in the mass degradation of RanGTPase
432 observed in the whole blood experiment shown in Figure 6. In this model, the assembly
433 modulator compound action can be thought of as serving as an external rather than internal
434 reboot of the cellular operating system. A future prediction to be tested, is that longer-term

435 treatment of blood results in complete normalization of RanGTPase – and restoration of
436 p62/SQSTM1 -- in the target complex present in PBMCs. By virtue of having therapeutic small
437 molecules as affinity ligands for target identification, the pathways discovered can be
438 productively illuminated by future studies, including by fractionation and reconstitution of
439 functional activities in extracts.
440
441 Second, these data, together with the studies shown previously, are consistent with the
442 hypothesis that, despite the heterogeneity of ALS clinical presentation and time course of
443 progression, there is a common underlying pathway that is the basis of the disease – and that
444 assembly modulators are therapeutic at that underlying shared level. While we hypothesize that
445 restoration of autophagy is a crucial part of this pathway, re-establishment of homeostasis likely
446 involves far more than just restoration of autophagy. In this regards the involvement of
447 miniscule subsets of the specific gene products found together in the target multi-protein
448 complex and the role of protein degradation, is notable. These targets could not have been
449 detected by powerful molecular biological tools such as CRISPR or siRNA knockdown studies,
450 because of the heterogeneous roles of small subsets of many, if not most, of the proteins
451 comprising the target multi-protein complex. Thus the concept of protein "moonlighting"[34,35]
452 may be more pervasive than is currently generally recognized. Conversely, the level of
453 organization of gene expression accessed by protein assembly modulation may be therapeutic
454 for diverse diseases in ways not generally appreciated today.
455

456 Finally, it should be noted that many if not most patients come to medical attention long
457 after the most effective period of treatment is lost. Drugs to stop the disease process may still
458 be effective, but rely on maintenance of the underlying framework of feedback loops to restore
459 homeostasis, once disease progression is arrested. Sometimes however, those feedback loops
460 fail and homeostasis is not restored, whether or not the primary disease process has been
461 blocked. We hypothesize ALS is one such example, making it extremely difficult to treat. The
462 methods described here provide a means of detecting ALS early, prior to onset of severe
463 disability, when it is most treatable – and provide a potentially effective treatment in the form
464 of the small molecule ligands themselves, that were used for disease detection. It is notable
465 that pt 78 came to medical attention early in her clinical course, prior to serious disability, and
466 yet, the signature changes (lowered p62 and elevated RanGTPase 17kDa fragment) were
467 nevertheless observed, and sadly, progressed with worsening of ALS, culminating in her death,
468 approximately 2 years after initial detection of the Ran 17kDa fragment as shown in Figure 5,
469 together with the reciprocal change in p62/SQSTM1, seen exacerbated over time. To date, these
470 findings have been observed in 13 of 13 ALS patients and are lacking in 4 of 6 healthy controls,
471 by the methods described. While the specificity of these signatures are relatively low, seen in 2
472 of 6 healthy controls, the high sensitivity implied by detection in 13 of 13 ALS patients, together
473 with the clinical history, make this diagnostic approach promising. PBMCs are a readily
474 accessible tissue. Used as affinity ligands, these small molecules could enable early diagnosis of
475 ALS, prior to extensive motor neuron death, when treatment would be more effective.
476 Remarkably, the same compounds, or their close analogs, may prove to be effective ALS
477 therapeutics.

478 **Methods**

479 **Preparation of PBMC extracts**[36]

480 Whole blood collected in purple-top EDTA tubes from healthy individuals or ALS patients under
481 Loma Linda Medical Center IRB# 5160136 was shipped at room temperature by overnight
482 courier to the San Francisco lab where it was diluted 1:1 with phosphate-buffered saline and
483 layered on ficoll and centrifuged for 15 minutes at 1,000 xg at room temperature with brake
484 off. PBMCs were collected at the interface, diluted with PBS 1:1 and centrifuged at 600 xg /15
485 minutes. The supernatant was aspirated and the pellet dissolved in p-body buffer (PBB)
486 consisting of 10mM Tris pH 7.5 ,10mM NaCl, 6mM MgAc, 1mM EDTA, and 0.35% Triton-X-100
487 and centrifuged at 4oC 10,000xg/10min. The 10kxg supernate was collected, aliquoted and
488 flash frozen in liquid nitrogen and stored at -80°C until use.

489

490 **Assembly modulator compounds**

491 Each assembly modulator chemotype is structurally quite different from one another,
492 depending on the target to which it is directed, the allosteric site involved, etc. The two ALS-
493 active assembly modulator chemotypes used here, typified by compounds PAV-073 and PAV-
494 667 are compared for drug-like properties in Table 2. The structure of PAV-073, a member of
495 the THIQ chemotype, and its modification to allow its use as an affinity ligand for drug resin
496 affinity chromatography or photocrosslinking, is described in reference 14.

497

498 **Drug Resin affinity chromatography**

499 A variation on the theme of methods described in previous publications was used here[14–16]. For
500 brain from wildtype or SOD1 mutant animals, tissue was homogenized in cold low salt buffer
501 (10mM HEPES pH 7.6, 10mM NaCl, 1mM MgAc with 0.35% Tritonx100) then centrifuged at
502 10,000 xg for 10 minutes at 4°C. The post-mitochondrial supernatant was adjusted to a
503 concentration of approximately 10 mg/ml and equilibrated in a physiologic column buffer (50
504 mM HEPES ph 7.6, 100 mM KAc, 6 mM MgAc, 1 mM EDTA, 4mM TGA). For DRAC of both MoBr
505 and human PBMC extracts, the 10k sup samples being compared were first normalized either by
506 absorbance at 280nm or by Coomassie brilliant blue or silver staining pattern. Samples were
507 then supplemented with an energy cocktail (to a final concentration of 1mM rATP, 1mM rGTP,
508 1mM rCTP, 1mM rUTP, and 5 µg/mL creatine kinase) in the presence of physiological salts
509 (50mM HEPES pH 7.6, 100mM Kac, MgAc 5mM, 1mM DTT) and incubated for one hour at either
510 4° C or 22° C degrees on 30 µl of affigel resin coupled to THIQ compound or a 4% agarose matrix
511 (control). The input material was collected after flow through the column and the resin was
512 then washed with 3 ml column buffer. The resins were eluted for 2 hours then overnight at 22°C
513 then 4°C in 100µl column buffer containing 100µM of the cognate compound. Eluates were run
514 on WB or sent for MS-MS for analysis.

515

516 **Chemical photocrosslinking**

517 A variation of protocols as published previously[14] was used. Extract from MoBr were prepared
518 as described above then adjusted to a protein concentration of approximately 3 mg/ml in
519 column buffer (Hepes pH 7.5 50mM, Kac 100mM, MgAc 5mM, DTT or TGA 1mM) containing

520 0.1% triton. 1% DMSO or 100µM PAV-073 was added to 6µl of extract, then 3µM of PAV-073
521 photocrosslinker or a negative control crosslinker (comprising of the biotin and diazirine
522 moieties without compound) were added. The extract was incubated for 20 minutes then
523 exposed to UV at 365nM wavelength for 10 minutes then left on ice for one hour. After
524 crosslinking, samples were divided in two 20 µl aliquots and one set was denatured by adding
525 20 µL of column buffer 4µl of 10% SDS, 0.5 µl 1M dithiothreitol (DTT), and heating to 100°C for 5
526 minutes. Both native and denatured aliquots were then diluted in 800 µl column buffer
527 containing 0.1% triton. 5 µl of magnetic streptavidin beads (Pierce) were added to all samples
528 and mixed for one hour at room temperature to capture all biotinylated proteins and co-
529 associated proteins. Samples were placed on a magnetic rack to hold the beads in placed and
530 washed three times with 800 µl of column buffer containing 0.1% triton. After washing, beads
531 were resuspended in 80 µl of gel loading buffer containing SDS and analyzed by SDS-PAGE
532 followed by transfer to PVDF membrane for WB.
533
534
535 **WB Procedure**
536 SDS-PAGE gels were transferred in Towbin buffer (25mM Tris, 192mM glycine, 20% w/v
537 methanol) to polyvinylidene fluoride membrane, blocked in 1% bovine serum albumin (BSA) in
538 PBS, incubated overnight at 4°C in a 1:1 dilution of 100µg/mL affinity-purified primary rabbit
539 IGG to PDI (Abcam 96744) in 1% BSA in PBS containing 0.1% Tween-20 (PBST). Membranes were
540 then washed twice in PBST and incubated for two hours at room temperature in a 1:5,000
541 dilution of secondary anti-rabbit or anti-mouse antibody coupled to alkaline phosphatase in

542 PBST. Membranes were washed two more times in PBST then incubated in a developer solution
543 prepared from 100 µL of 7.5 mg/mL 5-bromo-4-chloro-3-indolyl phosphate dissolved in 60%
544 dimethyl formamide (DMF) in water and 100µl of 15 mg/ml nitro blue tetrazolium dissolved in
545 70% DMF in water, adjusted to 50mL with 0.1 Tris (pH 9.5) and 0.1 mM magnesium chloride.
546 Membranes were scanned and the integrated density of protein band was measured on ImageJ.
547 Averages and the standard deviation between repeated experiments were calculated and
548 plotted on Microsoft Excel. Primary antibodies for RanGTPase (Abcam ab31118), p62/SQSTM1
549 (Abcam, ab56416), were used at 1:1,000 dilution by the same procedure. Secondary goat
550 antibodies to mouse (Abcam ab97020) or rabbit (Abcam ab6722) were used at 1:5,000 dilution.
551
552 **Tandem mass spectrometry**
553 Samples were processed by SDS PAGE using a 10% Bis-tris NuPAGE gel with the 2-(N-
554 morpholino)ethanesulfonic acid buffer system. The mobility region, including all proteins, was
555 excised and washed with 25 mM ammonium bicarbonate followed by 15mM acetonitrile.
556 Samples were reduced with 10 mM dithoithreitol and 60° C followed by alkylation with 50 mM
557 iodoacetamide at room temperature. Samples were then digested with trypsin (Promega)
558 overnight (18 hours) at 37° C then quenched with formic acid and desalted using an Empore SD
559 plate. Half of each digested sample was analyzed by LC-MS/MS with a Waters NanoAcquity
560 HPLC system interfaced to a ThermoFisher Q Exactive. Peptides were loaded on a trapping
561 column and eluted over a 75 µM analytical column at 350 nL/min packed with Luna C18 resin
562 (Phenomenex). The mass spectrometer was operated in a data dependent mode, with the

563 Oribtrap operating at 60,000 FWHM and 15,000 FWHM for MS and MS/MS respectively. The
564 fifteen most abundant ions were selected for MS/MS.
565
566 Data was searched using a local copy of Mascot (Matrix Science) with the following parameters:
567 Enzyme: Trypsin/P; Database: SwissProt Human (conducted forward and reverse plus common
568 contaminants); Fixed modification: Carbamidomethyl (C) Variable modifications: Oxidation (M),
569 Acetyl (N-term), Pyro-Glu (N-term Q), Deamidation (N/Q) Mass values: Monoisotopic; Peptide
570 Mass Tolerance: 10 ppm; Fragment Mass Tolerance: 0.02 Da; Max Missed Cleavages: 2. The data
571 was analyzed by spectral count methods.
572
573 **Diagnosis of ALS.** A diagnosis of ALS was made in all patients by a combination of their
574 neurological exam and their electrodiagnostic testing. The examination was required to reveal
575 signs of upper and lower motor neuron pathology. Although the phenotypic spectrum of ALS is
576 quite variable, upper and lower motor neuron signs were represented in all patients and a brief
577 phenotypic description is included in Table 1. Electrodiagnostic data included multifocal
578 evidence of denervation and reduced motor neuron recruitment.
579
580 **Whole blood incubation and analysis**. 100µl aliquots of EDTA-anticoagulated whole blood is
581 dispensed into 24 well plates containing 100µl of room temperature 80% PBS with 10mM
582 glucose and then treated with DMSO to 0.01% or drug in DMSO to the same dilution with final
583 concentration of 5µM drug. After 72hrs samples are collected and adjusted to 1% SDS. One
584 aliquot was prepared in gel loading buffer as starting material. Another aliquot added to energy

585 cocktail (1mM rNTPs with 0.2µg/ml CK, 50mM Hepes pH 7.6 100mK KAc, 6mM MgAc and 4mM
586 TGA) at total volume 100µl and incubated at 37°C for 1hr, and then prepared in gel loading
587 buffer. Samples were analyzed by SDS-PAGE and WB for full length RanGTPase.
588
589 **Statistics**
590 Graphs were generated and statistical analysis were preformed using GraphPad prism version
591 10.4.1. For Figure 3, unpaired t-tests were conducted to assess statistical significance in the
592 amount of protein bound to the THIQ resin for each starting material. In figure 6, a 2way ANOVA
593 was used, followed by Tukey's multiple comparisons tests. P-values of selected comparisons
594 were shown on the graph, including changes in RanGTPase levels before and after treatment
595 within each condition and differences in RanGTPase levels between DMSO and drug treatments
596 post-treatment. Statistical significance is indicated as follows: nsa ($P > 0.05$), * ($P \leq 0.05$), ** ($P \leq$
597 0.01), *** ($P \leq 0.001$), **** ($P \leq 0.0001$).
598
599 **Ethical Approval**
600 Whole blood collected in purple-top EDTA tubes from healthy individuals or ALS patients under
601 Loma Linda Medical Center IRB# 5160136
602
603
604
605
606

607 **References**

608 1. Al-Chalabi, A. & Hardiman, O. The epidemiology of ALS: a conspiracy of genes, environment
609 and time. *Nat. Rev. Neurol.* **9**, 617–628 (2013).
610 2. Chiò, A. *et al.* Prognostic factors in ALS: A critical review. *Amyotroph. Lateral Scler. Off. Publ.*
611 *World Fed. Neurol. Res. Group Mot. Neuron Dis.* **10**, 310–323 (2009).
612 3. Rizea, R. E., Corlatescu, A.-D., Costin, H. P., Dumitru, A. & Ciurea, A. V. Understanding
613 Amyotrophic Lateral Sclerosis: Pathophysiology, Diagnosis, and Therapeutic Advances. *Int. J.*
614 *Mol. Sci.* **25**, 9966 (2024).
615 4. Hernan-Godoy, M. & Rouaux, C. From Environment to Gene Expression: Epigenetic
616 Methylations and One-Carbon Metabolism in Amyotrophic Lateral Sclerosis. *Cells* **13**, 967
617 (2024).
618 5. Cabrera-Rodríguez, R. *et al.* TDP-43 Controls HIV-1 Viral Production and Virus Infectiveness.
619 *Int. J. Mol. Sci.* **24**, 7658 (2023).
620 6. Gandhi, J. *et al.* Protein misfolding and aggregation in neurodegenerative diseases: a review
621 of pathogeneses, novel detection strategies, and potential therapeutics. *Rev. Neurosci.* **30**,
622 339–358 (2019).
623 7. Grad, L. I., Rouleau, G. A., Ravits, J. & Cashman, N. R. Clinical Spectrum of Amyotrophic
624 Lateral Sclerosis (ALS). *Cold Spring Harb. Perspect. Med.* **7**, (2017).
625 8. Chou, C.-C. *et al.* TDP-43 pathology disrupts nuclear pore complexes and nucleocytoplasmic
626 transport in ALS/FTD. *Nat. Neurosci.* **21**, 228–239 (2018).

627 9. Baradaran-Heravi, Y., Van Broeckhoven, C. & van der Zee, J. Stress granule mediated protein
628 aggregation and underlying gene defects in the FTD-ALS spectrum. *Neurobiol. Dis.* **134**,
629 104639 (2020).
630 10. Gasset-Rosa, F. *et al.* Cytoplasmic TDP-43 De-mixing Independent of Stress Granules Drives
631 Inhibition of Nuclear Import, Loss of Nuclear TDP-43, and Cell Death. *Neuron* **102**, 339-
632 357.e7 (2019).
633 11. Kim, C. K. *et al.* Alzheimer's Disease: Key Insights from Two Decades of Clinical Trial Failures.
634 *J. Alzheimers Dis. JAD* **87**, 83–100 (2022).
635 12. Aggad, D., Vérièpe, J., Tauffenberger, A. & Parker, J. A. TDP-43 toxicity proceeds via calcium
636 dysregulation and necrosis in aging Caenorhabditis elegans motor neurons. *J. Neurosci. Off.*
637 *J. Soc. Neurosci.* **34**, 12093–12103 (2014).
638 13. Buratti, E. & Baralle, F. E. Multiple roles of TDP-43 in gene expression, splicing regulation,
639 and human disease. *Front. Biosci. J. Virtual Libr.* **13**, 867–878 (2008).
640 14. Yu, S. F. *et al.* Protein Assembly Modulation: A New Approach to Amyotrophic Lateral
641 Sclerosis (ALS) Therapeutics. *J. Exp. Neurol.* **5**, 210–230 (2024).
642 15. Michon, M. *et al.* A pan-respiratory antiviral chemotype targeting a transient host multi-
643 protein complex. *Open Biol.* **14**, 230363 (2024).
644 16. Lingappa, A. F. *et al.* Small molecule protein assembly modulators with pan-cancer
645 therapeutic efficacy. *Open Biol.* **14**, 240210 (2024).
646 17. Bechtel, W. & Bich, L. Situating homeostasis in organisms: maintaining organization through
647 time. *J. Physiol.* **602**, 6003–6020 (2024).
648 18. Tomkins, G. M. The metabolic code. *Science* **189**, 760–763 (1975).

649 19. Marty, L. *et al.* The NADPH-dependent thioredoxin system constitutes a functional backup
650 for cytosolic glutathione reductase in Arabidopsis. *Proc. Natl. Acad. Sci. U. S. A.* **106**, 9109–
651 9114 (2009).
652 20. Noble, D. From Genes to Whole Organs: Connecting Biochemistry to Physiology. in *Novartis*
653 *Foundation Symposia* (eds. Bock, G. R. & Goode, J. A.) vol. 239 111–128 (Wiley, 2001).
654 21. Pardee, A. B. Regulatory Molecular Biology. *Cell Cycle* **5**, 846–852 (2006).
655 22. Pardee, A. B. & Reddy, G. P.-V. Beginnings of feedback inhibition, allostery, and multi-protein
656 complexes. *Gene* **321**, 17–23 (2003).
657 23. Fenton, A. W. Allostery: an illustrated definition for the 'second secret of life'. *Trends*
658 *Biochem. Sci.* **33**, 420–425 (2008).
659 24. Müller-Schiffmann, A. *et al. A Pan-Respiratory Antiviral Chemotype Targeting a Transient*
660 *Host Multiprotein Complex*. http://biorxiv.org/lookup/doi/10.1101/2021.01.17.426875
661 (2021) doi:10.1101/2021.01.17.426875.
662 25. Lingappa, A. F. *et al.* Small Molecule Assembly Modulators with Pan-Cancer Therapeutic
663 Efficacy. *bioRxiv* 2022.09.28.509937 (2022) doi:10.1101/2022.09.28.509937.
664 26. Nardo, G. *et al.* Amyotrophic lateral sclerosis multiprotein biomarkers in peripheral blood
665 mononuclear cells. *PloS One* **6**, e25545 (2011).
666 27. Luotti, S. *et al.* Diagnostic and prognostic values of PBMC proteins in amyotrophic lateral
667 sclerosis. *Neurobiol. Dis.* **139**, 104815 (2020).
668 28. Pongrácová, E., Buratti, E. & Romano, M. Prion-like Spreading of Disease in TDP-43
669 Proteinopathies. *Brain Sci.* **14**, 1132 (2024).

670 29. Duyckaerts, C., Clavaguera, F. & Potier, M.-C. The prion-like propagation hypothesis in
671 Alzheimer's and Parkinson's disease. *Curr. Opin. Neurol.* **32**, 266–271 (2019).
672 30. Wenzhi, Y., Xiangyi, L. & Dongsheng, F. The prion-like effect and prion-like protein targeting
673 strategy in amyotrophic lateral sclerosis. *Heliyon* **10**, e34963 (2024).
674 31. Feng Yu, S. *et al. Protein Assembly Modulation: A New Approach to ALS Therapeutics*.
675 http://biorxiv.org/lookup/doi/10.1101/2023.07.24.550252 (2023)
676 doi:10.1101/2023.07.24.550252.
677 32. Dervishi, I. *et al.* Protein-protein interactions reveal key canonical pathways, upstream
678 regulators, interactome domains, and novel targets in ALS. *Sci. Rep.* **8**, 14732 (2018).
679 33. Kanehisa, M., Furumichi, M., Sato, Y., Kawashima, M. & Ishiguro-Watanabe, M. KEGG for
680 taxonomy-based analysis of pathways and genomes. *Nucleic Acids Res.* **51**, D587–D592
681 (2023).
682 34. Copley, S. D. Moonlighting is mainstream: paradigm adjustment required. *BioEssays News*
683 *Rev. Mol. Cell. Dev. Biol.* **34**, 578–588 (2012).
684 35. Jeffery, C. J. Multitalented actors inside and outside the cell: recent discoveries add to the
685 number of moonlighting proteins. *Biochem. Soc. Trans.* **47**, 1941–1948 (2019).
686 36. Jia, Y. *et al.* A Modified Ficoll-Paque Gradient Method for Isolating Mononuclear Cells from
687 the Peripheral and Umbilical Cord Blood of Humans for Biobanks and Clinical Laboratories.
688 *Biopreservation Biobanking* **16**, 82–91 (2018).
689
690
691

Supplemental Figure 1.

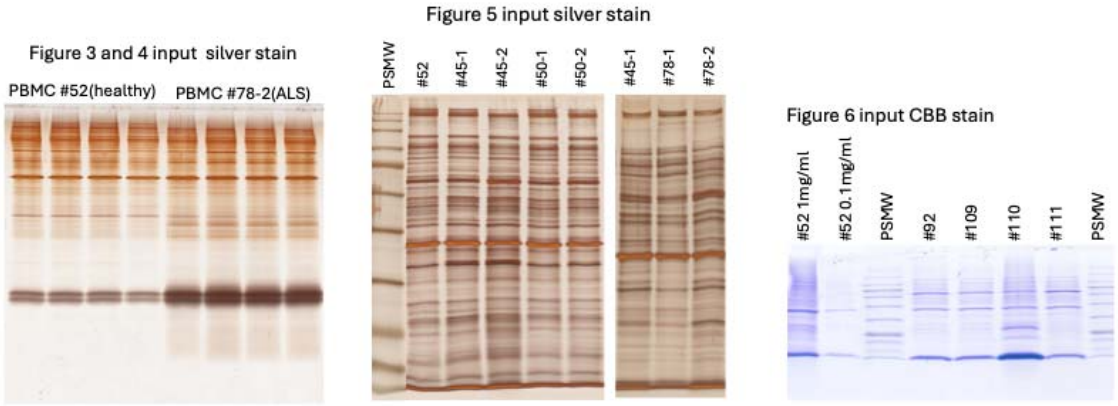

Legend to Supplemental Figure 1. Input extracts for Figures 3-6. Silver stain (left and middle panels) and CBB stain (right panel) of input extracts used for DRAC (Figure 3 and 5), photocrosslinking (Figure 4), and RanGTPase degradation (Figure 6) assays.

692

693

694

695

696

697

698

699

700

701

702

703

704

Supplemental Figure 2.

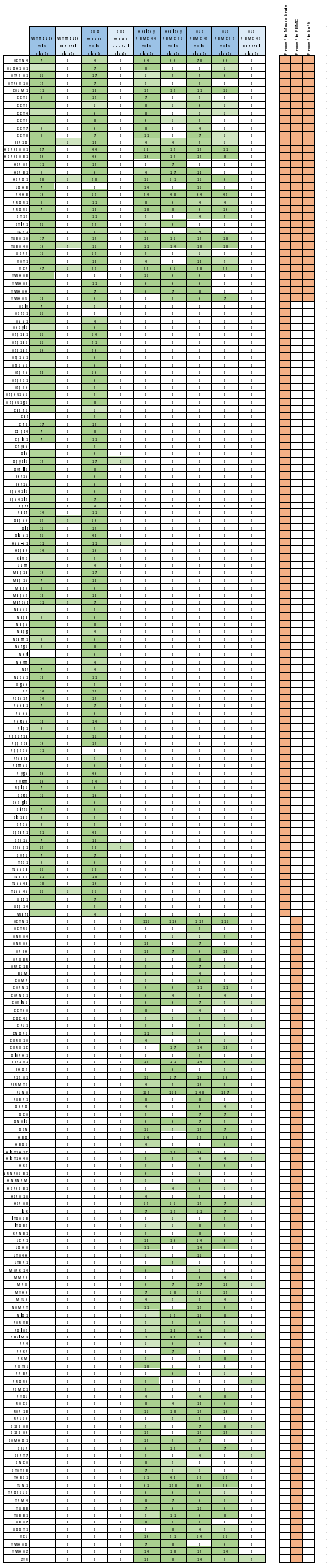

Legend to Supplemental Figure 2. Spectral counts for entire dataset of MoBr and PBMC THIQ resin eluates. Colors represent the number of spectral counts for a given protein in each sample, ranging from light green (low counts) to dark green (high counts). The right panel indicates whether a given protein was in one of both of the datasets, according to threshold values of >4 spectral counts in the drug eluate and <4 spectral counts in the control column eluate.

707 **Supplemental Figure 3.**

708

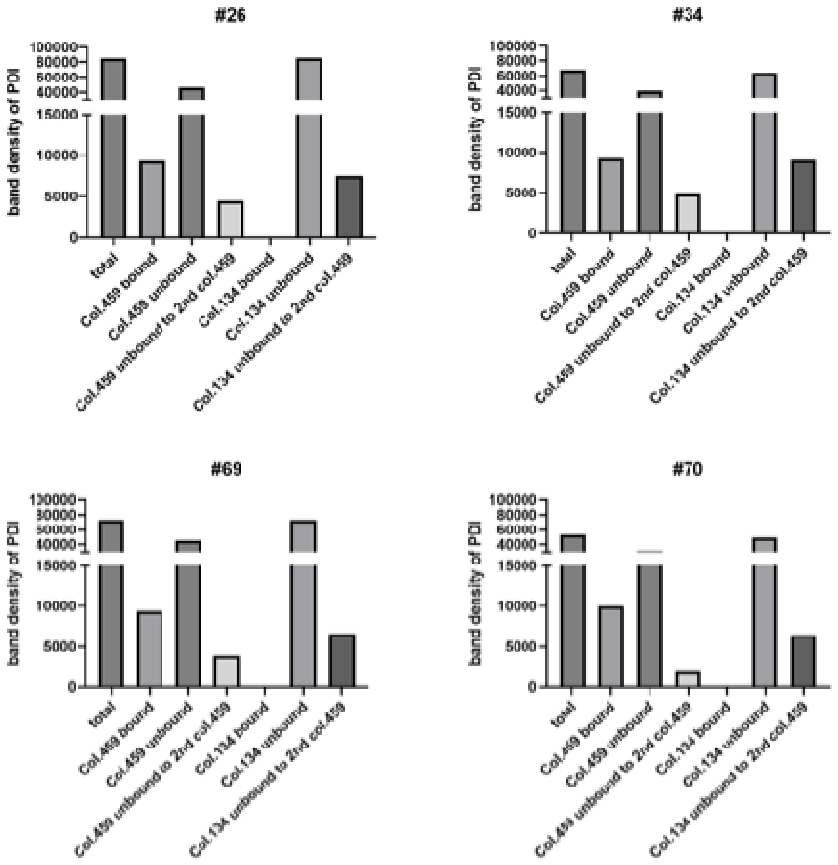

709

710 Legend to Supplemental Figure 3. Confirmation that only a small subset of PDI is present in the DRAC-
711 identified target and that very little additional pre-existing PDI is competent for formation of new target
712 without *de novo* synthesis. PBMC extracts were prepared as previously, applied to drug resins and bound
713 proteins analyzed by WB for PDI. The band corresponding to the correct molecular weight was
714 quantified as shown. Samples from three ALS patients and one healthy control are shown. Column 459
715 represents the THIQ drug resin and column 134 the control drug resin. As can be seen, approximately
716 10% of PDI is in the complex bound to the drug resin in all cases, with no significant binding to the
717 control resin in any case. The flowthrough from the first column (drug or control) was applied to a
718 second copy of the drug resin, demonstrating substantial depletion from the first column and that,

719 despite losses, a substantial fraction of the flow through from the control column remains competent to

720 bind to the drug resin column.

721

722 **Abbreviations**

723 ALS – Amyotrophic Lateral Sclerosis

724 BSA – bovine serum albumin

725 CFPSA – Cell-free protein synthesis and assembly

726 Col – column

727 Ctrl - control

728 CNS – Central Nervous System

729 DTT - dithiothreitol

730 DRAC – drug resin affinity chromatography

731 Dx - diagnosis

732 eDRAC – energy-dependent drug resin affinity chromatography

733 FTD – Fronto-Temporal Dementia

734 H – healthy individual

735 HEPES – 4-(2-hydroxyethyl)-1-piperazineethanesulfonic acid

736 IND – investigational new drug

737 LMN – lower moter neuron

738 MoBr – mouse brain

739 MS-MS – tandem mass spectrometry

740 ns – non-significant

741 PBMC – Peripheral blood mononuclear cell

742 PBS – phosphate-buffered saline

743 PDF – patient-derived fibroblast

744 PDI – protein disulfide isomerase

745 PTM – post-translationally modified

746 PSMW – Prestained molecular weight markers

747 PVDF - polyvinylidene difluoride

748 SAP – streptavidin precipitation

749 SDS-PAGE – polyacrylamide gel electrophoresis in sodium dodecyl sulfate

750 TDP-43 – Transactive Response DNA-binding Protein 43

751 TGA – thioglycolic acid

752 TPP – target product profile

753 UMN – upper motor neuron

754 WB – western blot

755 * - p value < 0.05

756 ** - p value < 0.01

757 *** - p value < 0.001

758 **** - p value < 0.0001

759

760 **Dataset**

761 The relevant dataset has been submitted to the DRYAD database and can be accessed upon

762 publication at the following: DOI: 10.5061/dryad.0rxwdbsbm

763

764 **Competing Interests**

765 VRL is CEO and AFL COO of Prosetta Biosciences

766

767 **Funding Statement**

768 This work was supported by Target ALS (grant# IL-2023-C4-L1), DOD CDMRP (grant #.

769 W81XWH2210721), and Prosetta Biosciences.

770

771 **Acknowledgements**

772 We thank David Hanzel and the anonymous reviewers for careful reading of the manuscript and

773 numerous helpful suggestions.